Crystal Structure of a Rigid Ferrocene-Based Macrocycle from High-Resolution X-ray Powder Diffraction

Robert E. Dinnebier,*,† Li Ding,‡ Kuangbiao Ma,‡ Markus A. Neumann,§ Noppawan Tanpipat,§ Frank J. J. Leusen,§ Peter W. Stephens,⊥ and Matthias Wagner*,‡

Max-Planck-Institute for Solid State Research, Heisenbergstrasse 1, D-70569 Stuttgart, Germany, Institut für Anorganische Chemie, J.W. Goethe-Universität Frankfurt, Marie-Curie-Strasse 11, D-60439 Frankfurt (Main), Germany, Molecular Simulations Ltd., 230/250 The Quorum, Barnwell Road, Cambridge CB5 8RE, England, and Department of Physics and Astronomy, SUNY at Stony Brook, Stony Brook, New York 11974

Received June 12, 2001

A macrocycle, **6**, has been synthesized in high yield from 2,5-di(pyrazol-1-yl)hydroquinone and 1,1′-fc[B(Me)NMe_2]$_2$ {fc = Fe(C_5H_4)$_2$}. The molecule incorporates two redox-active 1,1′-ferrocenylene units in its backbone and contains four chiral boron centers, each of them possessing the same configuration. It is demonstrated that crystal structures of organometallics of moderate complexity can be solved from high-resolution X-ray powder diffraction patterns, once the connectivity between the functional groups is known.

Introduction

Polymeric materials and macrocyclic molecules containing redox-active functionalities are of considerable current interest. In the latter case, one major goal is to develop novel complexing agents and molecular receptors, capable of binding selectively a given substrate and mimicking biological processes.[1] Other applications lie in the fields of chemical sensors[2] and molecular electronics.[3] Among the redox-responsive units that are most extensively used, the organometallic complex ferrocene plays a particularly prominent role. The ferrocene moieties can be either attached to or incorporated within a macrocyclic framework. A variety of macrocyclic complexes with pendent ferrocene substituents are known to date. In contrast, those involving ferrocene fragments as integral parts of the molecular architecture are still relatively rare, since their generation is met with considerable synthetic challenges.[4]

Exploiting the self-assembly of B−N and B−O bonds, our group has recently initiated a novel approach to organometallic macromolecules. The aim of our research is to synthesize metal-containing polymers as well as cyclic frameworks. Inspired by the work of Stoddart on "molecular squares",[5] we have already investigated the reaction of difunctional Lewis bases (e.g., pyrazine; 4,4′-bipyridine) and 1,1′-diborylated ferrocenes, which, however, led to polymeric materials.[6−8] No formation of macrocyclic structures was observed. To study the factors governing polymer assembly on one hand and macrocycle formation on the other, we decided to replace the monodentate Lewis bases used so far by chelating ligands. 2,5-Di(pyrazol-1-yl)hydroquinone,[9,10] **1**, appeared to be well-suited, since its reaction with the monoborylated ferrocene **2**[11] gives the dinuclear complex **3** in high yield under very mild conditions (Scheme 1).[12] The purpose of this paper is to investigate whether treatment of the corresponding 1,1′-diborylated ferrocene **4** with **1** under similar reaction conditions will lead to polymer **5** or to macrocycle **6** (Scheme 2).

Results and Discussion

Synthesis and Characterization. The reaction of **1** and **4** in CH_2Cl_2 at ambient temperature results in the gradual liberation of $HNMe_2$, accompanied by the precipitation of a yellow microcrystalline solid. Its ^{1}H

* Corresponding authors. (R.E.D.) E-mail: R.Dinnebier@fkf.mpg.de. Fax: +49 711 689 1502. (M.W.) E-mail: Matthias.Wagner@chemie.uni-frankfurt.de. Fax: +49 69 798 29260.
† Max-Planck-Institute for Solid State Research.
‡ J.W. Goethe-Universität Frankfurt.
§ Molecular Simulations Ltd.
⊥ SUNY at Stony Brook.

(1) Beer, P. D.; Gale, P. A. *Angew. Chem., Int. Ed. Engl.* **2001**, *40*, 486.
(2) Edmonds, T. E. In *Chemical Sensors*; Edmonds, T. E., Ed.; Blackie: Glasgow, 1988.
(3) Vögtle, F. *Supramolecular Chemistry*; Wiley: Chichester, 1991.
(4) Hall, C. D. In *Ferrocenes*; Togni, A., Hayashi, T., Eds.; VCH: Weinheim, 1995. For a recent example see: López-Torres, M.; Fernández, A.; Fernández, J. J.; Suárez, A.; Castro-Juiz, S.; Vila, J. M.; Pereira, M. T. *Organometallics* **2001**, *20*, 1350.
(5) Slawin, A. M. Z.; Spencer, N.; Stoddart, J. F.; Williams, D. J. *Angew. Chem., Int. Ed. Engl.* **1988**, *27*, 1547.
(6) (a) Fontani, M.; Peters, F.; Scherer, W.; Wachter, W.; Wagner, M.; Zanello, P. *Eur. J. Inorg. Chem.* **1998**, 1453. (b) Fontani, M.; Peters, F.; Scherer, W.; Wachter, W.; Wagner, M.; Zanello, P. *Eur. J. Inorg. Chem.* **1998**, 2087.
(7) Grosche, M.; Herdtweck, E.; Peters, F.; Wagner, M. *Organometallics* **1999**, *18*, 4669.
(8) Dinnebier, R. E.; Wagner, M.; Peters, F.; Shankland, K.; David, W. I. F. *Z. Anorg. Allg. Chem.* **2000**, *626*, 1400.
(9) Catalán, J.; Fabero, F.; Guijarro, M. S.; Claramunt, R. M.; Maria, M. D. S.; Foces-Foces, M. d. l. C.; Cano, F. H.; Elguero, J.; Sastre, R. *J. Am. Chem. Soc.* **1990**, *112*, 747.
(10) Cornago, P.; Escolástico, C.; María, M. D. S.; Claramunt, R. M.; Carmona, D.; Esteban, M.; Oro, L. A.; Foces-Foces, C.; Llamas-Saiz, A. L.; Elguero, J. *J. Organomet. Chem.* **1994**, *467*, 293.
(11) Renk, T.; Ruf, W.; Siebert, W. *J. Organomet. Chem.* **1976**, *120*, 1.
(12) Ding, L.; Fabrizi de Biani, F.; Bolte, M.; Zanello, P.; Wagner, M. *Organometallics* **2000**, *19*, 5763.

10.1021/om0105066 CCC: $20.00
Publication on Web 11/22/2001

Scheme 1

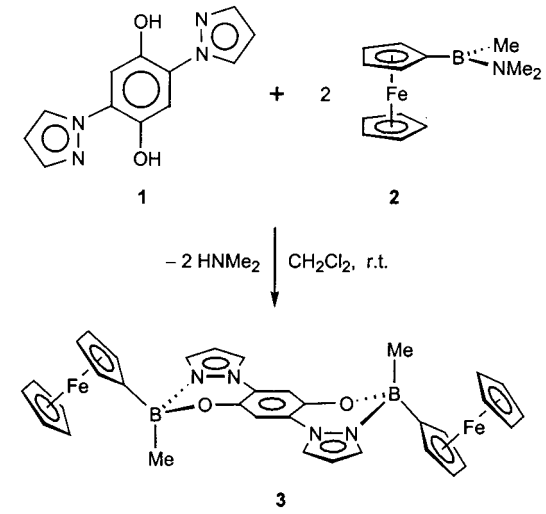

Scheme 2

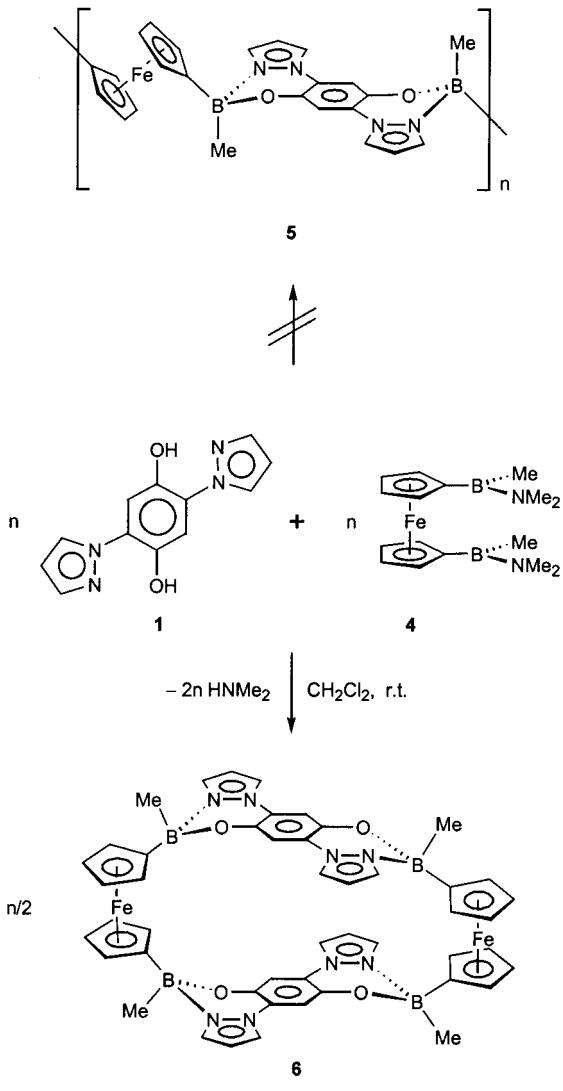

NMR spectrum in DMSO solution presents four signals for the pyrazolyl and hydroquinone fragments, indicating a high symmetry of the molecule in solution. The ferrocenyl moieties give rise to four resonances with equal integral values. A possible explanation would be that each of the four protons of a given C_5H_4 ring is placed in its own unique magnetic environment due to the close vicinity of a chiral tetracoordinate boryl substituent. Alternatively, the reaction product might contain two kinds of magnetically nonequivalent cyclopentadienyl rings. Experimental evidence counting against the first explanation is provided by the ^{1}H NMR spectrum of **3**,[12] which presents only two resonances for the substituted cyclopentadienyl ring. The second explanation, on the other hand, is supported by the solid state structure of the material (vide infra; however, one has to take into account that the average geometry of the molecule in solution might well possess a higher symmetry). A signal pattern very similar to the ^{1}H NMR spectrum is observed in the ^{13}C NMR spectrum. No signals of minor intensity, which might be attributed to the end groups of short oligomers, were detected. This leads to the conclusion that the reaction product consists either of long polymeric chains or of cyclic molecules. ESI-MS spectrometry, well-known to be a particularly mild tool for the investigation of fragile macromolecules, showed no peaks of masses higher than $m/z = 952$ [100%; high intensity]. It can thus safely be assumed that the main product of our reaction is the cyclic dimer **6** ($m/z = 952$) rather than the polymer **5**. **6** was preliminarily investigated by cyclic voltammetry. The single-step ferrocene oxidation possesses features of chemical reversibility. The redox potential ($E_0' = +0.02$ V, vs SCE) lies in the range frequently observed for ferrocenes bearing two tetracoordinate boron substituents.[6] The iron centers appear to be electronically noncommunicating. Controlled potential coulometric measurements failed due to severe poisoning of the electrode. For the same reason, the redox behavior of the hydroquinone fragments could not be elucidated.

Numerous attempts to grow single crystals of **6** failed, partly due to the poor solubility of the compound in all common solvents. Its crystal structure was therefore determined by high-resolution X-ray powder diffraction (Figure 1).

Structure Determination. The sample was mounted in transmission geometry in a 0.7 mm glass capillary (Hilgenberg, glass No. 50) and spun during measurement to reduce preferred orientation and grain size effects. The calculated absorption at this wavelength was low enough, making an absorption correction unnecessary. The crystal structure of **6** was solved with the software package Powder Solve[13] implemented in the Cerius^2 modeling environment version 4.2 MS.[14] By repeating Pawley refinement[15] for different space group symmetries, it was established that *C*2, *Cm*, *Cc*, *C*2/*m*, and *C*2/*c* were the only space groups likely to solve the crystal structure. All other monoclinic space groups could be ruled out on the basis of missing peaks or the presence of several symmetry-allowed reflections without intensity. Taking into account density constraints, it was concluded that there had to be eight ligand$-Fe^{2+}$ pairs in the unit cell, with one pair per asymmetric unit in *C*2/*m* and *C*2/*c* and two pairs per asymmetric unit in *C*2, *Cm*, and *Cc*.

(13) Engel, G. E.; Wilke, S.; König, O.; Harris, K. D. M.; Leusen, F. J. J. *J. Appl. Crystallogr.* **1999**, *32*, 1169.
(14) Cerius^2, DMol^3, and Materials Studio are products of Molecular Simulations Incorporated, 9685 Scranton Road, San Diego, CA 92121-3752.
(15) Pawley, G. S. *J. Appl. Crystallogr.* **1981**, *14*, 357.

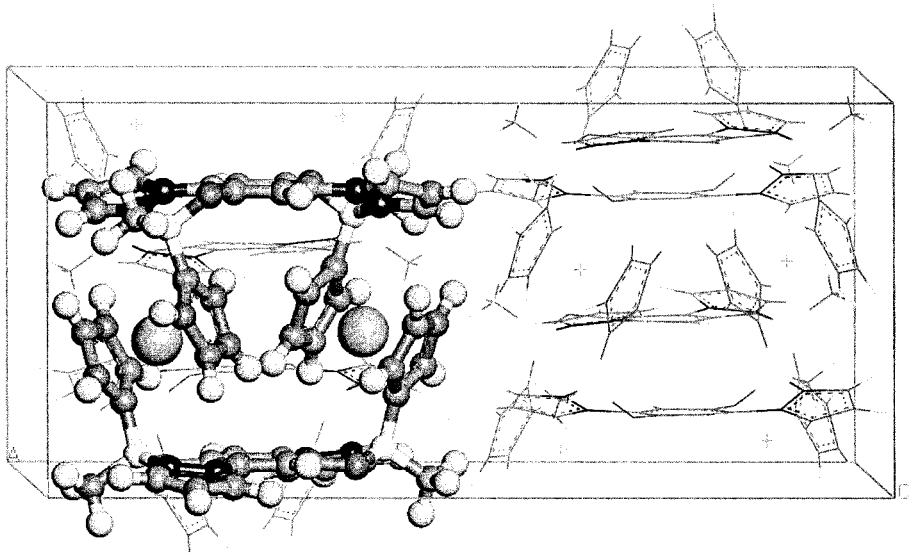

Figure 1. Crystal structure of **6** in a projection down the *a*-axis. A cyclic dimer containing two ferrocenylene units has been enhanced for clarity.

To solve crystal structures, Powder Solve makes use of a direct space approach. Thousands of trial structures are generated by a Monte Carlo/simulated annealing algorithm.[16] For each trial structure, a powder diffraction pattern is calculated, using background parameters and profile parameters that are determined by Pawley refinement prior to structure solution. The Monte Carlo/simulated annealing algorithm seeks to minimize the weighted Rietveld parameter R_{wp}[17] that measures the disagreement between the calculated and the experimental powder pattern. All molecules in the asymmetric unit are treated as motion groups for which internal torsional degrees of freedom can be defined. The positions and orientations of motion groups as well as the flexible torsions are the only degrees of freedom that are varied during the structure search.

In the crystal structure with the lowest R_{wp} value, a dimer motif was clearly recognizable, but it proved necessary to make some manual readjustment to obtain acceptable distances between the cyclopentadienyl moieties and the remaining parts of the ligands. From the comparison between the calculated and the experimental powder patterns, it was almost certain at this point that the crystal structure had been solved, but also that further structure refinement was essential.

Structure Refinement by First-Principles DFT. Using direct space approaches, increasingly complex crystal structures can be solved directly from powder diffraction data. In most cases, further refinement is required after structure solution, and it appears to be a general problem that powder diffraction patterns frequently do not contain enough information for a detailed structure refinement. Lattice energy minimizations using DFT (density functional theory) calculations can provide a convenient way out of this dilemma. Only the atomic coordinates have to be optimized, since accurate unit cell parameters can easily be extracted from the powder diffraction pattern by Pawley refinement. After lattice energy minimization, the agreement between the simulated and the experimental powder patterns can be improved by Rietveld refinement with fixed atomic coordinates, eventually enabling the refinement of a limited number of structural parameters.

DFT calculations and methods for structure determination from powder data are highly complementary. Structure solution techniques make it possible to pick the correct configuration of molecules out of a wide range of possibilities, the number of which can then be considerably reduced by DFT lattice energy minimizations. In cases where structure solution techniques find more than one acceptable crystal structure, DFT calculations can be used to identify the true structure solution, the correct crystal structure being the one that offers the best agreement with the experimental powder pattern after lattice energy minimization. All DFT calculations are based on a certain number of approximations, and it has to be checked that lattice energy optimizations are carried out at an appropriate level of theory. Comparing the powder pattern of the optimized crystal structure to the experimental one, the adequacy of the chosen method of calculation can be easily verified.

In this study, the structure refinement of complex **6** illustrates the applicability of high-level DFT calculations to structure refinement. All calculations were carried out with the program DMol^3 v4.2.1, using the nonlocal BP functional for the exchange correlation,[18] the DND basis set[19] in conjunction with relativistic effective core potentials for metal atoms, and thermal occupation of 0.005 au. Calculations were performed on periodic structures at the Γ-point with a real space cutoff of 4.0 Å. The optimized structures were taken as input for Rietveld refinement with Reflex, a software module that is implemented in Materials Studio.[14] Various parameters were adjusted by Rietveld refinement, including cell parameters, a global isotropic temperature

(16) Van Laarhoven, P. J. M.; Aarts, E. H. L. *Simulated Annealing: Theory and Applications*, D. Reidel Publishing Company: Dordrecht, 1987.

(17) Langford, I.; Louër, D. *Rep. Prog. Phys.* **1996**, *59*, 131. Hill, R. J.; Cranswick, L. M. D. *J. Appl. Crystallogr.* **1994**, *27*, 802.

(18) Becke, A. D. *Phys. Rev.* **1988**, *A38*, 3098. Wang, Y.; Perdew, J. P. *Phys. Rev.* **1991**, *B44*, 13298.

(19) Baldinozzi, J.; Berar, J. F. *J. Appl. Crystallogr.* **1993**, *26*, 128.

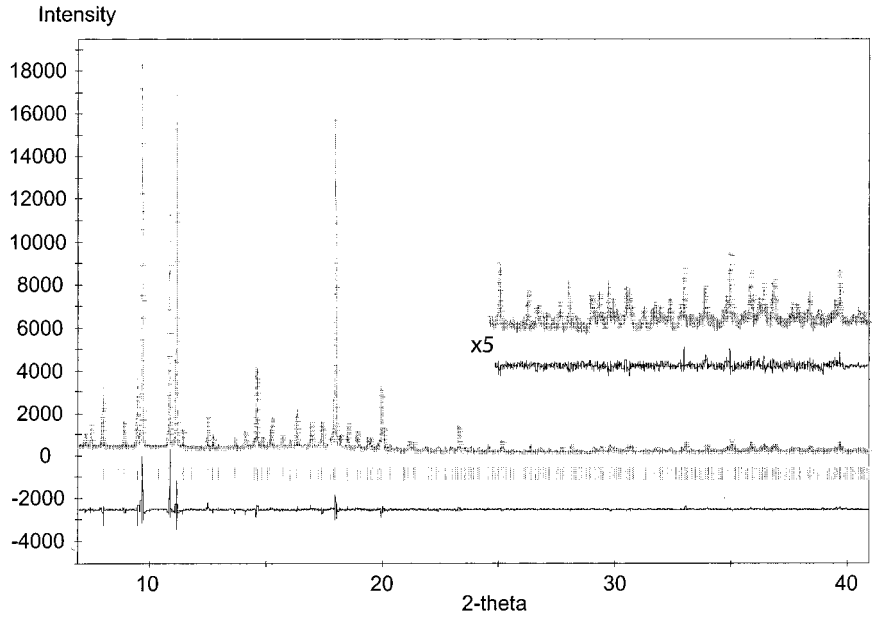

Figure 2. Scattered X-ray intensity for **6** at ambient conditions as a function of the diffraction angle 2θ. Shown are the observed pattern (diamonds), the best Rietveld fit profile (line), the reflection positions, and the difference curve between observed and calculated profiles as the trace at the bottom. The inset shows the high-angle part enlarged by a factor of 5 starting at 25° 2θ. The wavelength was $\lambda = 1.14991(2)$ Å. The weighted profile *R*-factor is 7.7%.

factor, the zero-point shift of the diffraction pattern, 20 background parameters, five parameters related to the Pseudo-Voigt peak profile, and four parameters related to the Berar−Baldinozzi asymmetry correction.[19] The angular range from 7° to 42.5° was chosen for Rietveld refinement, neglecting the first diffraction peak at around 5.4° because of its strong asymmetry.

In a first step, the structure of an isolated dimer was optimized with DMol^3 v4.2.1, starting from the geometry obtained by structure solution. The structure optimization was performed with medium convergence criteria (energy, 1×10^{-5} hartree; gradient, 1×10^{-3} hartree/bohr; displacement, 1×10^{-3} bohr) on a RS/6000 44P Model 270 IBM workstation with four Power3-II 375 MHz processors, requiring a total of 1.3 days of CPU time using all processors. Unlike the starting structure, the optimized dimer showed a 2-fold symmetry axis, and putting the dimer back into the crystal structure, it was realized that the true symmetry of the crystal was not *Cc* but *C*2/*c*. Defining the entire dimer as a motion group without internal degrees of freedom, a rigid body Rietveld refinement was carried out and an R_{wp} value of 10.59% was obtained. This value has to be compared to an R_{wp} factor of 6.61% resulting from Pawley refinement. Since all peak intensities are treated as independent parameters in Pawley refinement, the R_{wp} value obtained by Pawley refinement defines a lower limit for the results achieved by Rietveld refinement.[20]

In a second step, the crystal structure was further improved by a DFT optimization of a full unit cell. To save CPU time, the C-centered monoclinic cell was reduced to a primitive unit cell containing 132 non-hydrogen atoms in a volume of 2076 Å^3. The lattice energy optimization was carried out with coarse convergence criteria (energy, 2×10^{-5} hartree; gradient, 1×10^{-2} hartree/bohr; displacement, 1×10^{-2} bohr) on an RS/6000 44P Model 170 IBM workstation with four Power3-II 333 MHz processors, requiring 4.3 days of CPU time using all processors. For the optimized crystal structure, Rietveld refinement with fixed atomic coordinates resulted in an R_{wp} value of 8.03%.

Finally, a rigid body Rietveld refinement was carried out with the ligands and the Fe^{2+} ions being defined as independent motion groups. The torsion angles describing the rotation of the cyclopentadienyl moieties with respect to the remaining parts of the ligands were also adjusted. The rigid body Rietveld refinement slightly reduced the R_{wp} factor to 7.66% and resulted in minor structural changes, the mean square displacement including hydrogen atoms being 0.047 Å compared with the crystal structure determined by DFT. The crystal structure obtained at this point was accepted as the final result of the structure determination, since any further attempts to reduce the R_{wp} value by increasing the number of structural degrees of freedom led to unreasonable bond lengths or bond angles. Figure 1 shows the crystal structure of complex **6**. A comparison between the calculated and the experimental powder patterns is presented in Figure 2.

Crystal data of **6** are given in Table 1, and structural parameters and a selection of bond lengths and angles are summarized in Tables 2 and 3.

The hydroquinone ligand **1** and the monoborylated ferrocene **2** give the dinuclear complex **3** in its *trans*-configuration. The molecular structure of **3** was determined by single-crystal X-ray diffraction.[12] A subsequent analysis of the entire sample using X-ray powder diffraction did not show any indications for the presence of a second phase (i.e., microcrystals of **3** in its *cis*-configuration). Given this background, we initially expected the reaction between **1** and **4** to yield the polymer **5** rather than **6**, because the seemingly preferred *trans*-configuration at the hydroquinone linkers is not compatible with a cyclic molecular framework. In contrast to these a priori expectations, compound **6**

(20) Rietveld, H. M. *J. Appl. Crystallogr.* **1969**, *2*, 65.

Table 1. Crystallographic Data for 6

formula	$C_{48}H_{44}B_4Fe_2N_8O_4$
temp [K]	295
fw [g/mol]	952.87
space group	*C*2/*c*
a [Å]	14.932(5)
b [Å]	11.466(3)
c [Å]	24.556(8)
β [Å]	98.97(3)
V [Å^3]	4152.8
Z	4
D_{calc} [g cm^{-3}]	1.524
μ [cm^{-1}] (100% packing)	27.07
2θ range [deg]	2−42.5
step size [°2θ]	0.005
counting time/step [s]	4.0
wavelength [Å]	1.14991(2)

Table 2. Positional Parameters, U_i [Å^2 × 10^3], of 6 in *C*2/*c* at 295 K[a]

atom	*x*/*a*	*y*/*b*	*z*/*c*	atom	*x*/*a*	*y*/*b*	*z*/*c*
Fe1	0.1228	0.4111	0.3773	H1	0.2588	0.0338	0.2518
C1	0.0863	0.0890	0.2801	H2	0.3902	0.0256	0.3425
C2	0.2539	0.0514	0.2946	H3	0.2997	0.0784	0.4290
C3	0.3194	0.0472	0.3411	H4	0.1364	−0.0520	0.4460
C4	0.2741	0.0723	0.3854	H5	0.0549	0.0337	0.4725
C5	0.1181	0.0380	0.4550	H6	0.1704	0.0715	0.4878
C6	0.2642	0.7292	0.4093	H7	0.2639	0.8202	0.4236
C7	0.0977	0.2542	0.4153	H8	0.3243	0.7192	0.3890
C8	0.1645	0.3213	0.4505	H9	0.2343	0.2953	0.4640
C9	0.1264	0.4311	0.4626	H10	0.1622	0.5022	0.4857
C10	0.0351	0.4341	0.4347	H11	−0.0116	0.5065	0.4353
C11	0.0180	0.3262	0.4057	H12	−0.0451	0.3026	0.3798
C12	0.2089	0.3794	0.3214	H13	0.2459	0.2984	0.3203
C13	0.1185	0.3983	0.2942	H14	0.0775	0.3355	0.2682
C14	0.0916	0.5119	0.3092	H15	0.3016	0.4950	0.3794
C15	0.1650	0.5665	0.3453	H16	0.0252	0.5494	0.2956
C16	0.2374	0.4823	0.3525	H17	−0.1173	0.8369	0.3812
C17	0.0113	0.0889	0.3086	H18	−0.0455	0.7796	0.4880
C18	0.0037	0.7820	0.3066	H19	0.1254	0.7032	0.4803
C19	0.0857	0.7820	0.2847	H20	0.2748	0.6722	0.4458
C20	−0.0526	0.7989	0.3977	H21	−0.1333	0.0930	0.2991
C21	−0.0149	0.7709	0.4511	H22	−0.1425	0.7738	0.2895
C22	0.0726	0.7316	0.4478				
C23	−0.0754	0.0922	0.2773				
C24	−0.0798	0.7804	0.2726				
B1	0.1033	0.1181	0.4004				
B2	0.1738	0.6992	0.3669				
N1	0.1738	0.0792	0.3112				
N2	0.1860	0.0914	0.3670				
N3	0.0100	0.7755	0.3645				
N4	0.0871	0.7342	0.3954				
O1	0.0193	0.0782	0.3635				
O2	0.1667	0.7803	0.3175				

[a] All temperature factors are constrained to be equal within the molecule with U_i = 25 [Å^2 × 10^3].

Table 3. Selected Bond Lengths [Å], Angles [deg], and Torsion Angles [deg] of 6[a]

Fe−C(Cp)	2.03−2.08
Fe−COG(Cp)	1.65, 1.69
C(Cp)−C(Cp)	1.43, 1.44
B−N	1.62
B−O	1.52
B−C	1.61
N(1)−N(2)	1.36
Fe···Fe intramolecular	6.74
Fe···Fe intermolecular	7.57
H···H min (intramolecular)	2.25
B−COG(Cp)−Fe	94.8, 95.0
C(7)−B(1)−N(2)	111.8
C(15)−B(2)−N(4)	110.4
N(2)−B(1)−B(2)−N(4)	175.7
C(5)−B(1)−B(2)−C(6)	37.5
C(8)−C(7)−B(1)−N(2)	−63.7
C(14)−C(15)−B(2)−N(4)	54.0
COG(Py)−C−C*− COG(Py*)	−56.6, 65.9
B(1)−COG(Cp)−COG(Cp*)−B(2)	−172.0

[a] Realistic standard deviations according to ref 17 are on the order of 1° for the angles and 0.05 [Å] for the bond lengths. COG(Cp) and COG(Py): centers of gravity of the cyclopentadienyl and the pyrazolyl rings. C−C* refers to the axes running through C1−C1 and C18−C18.

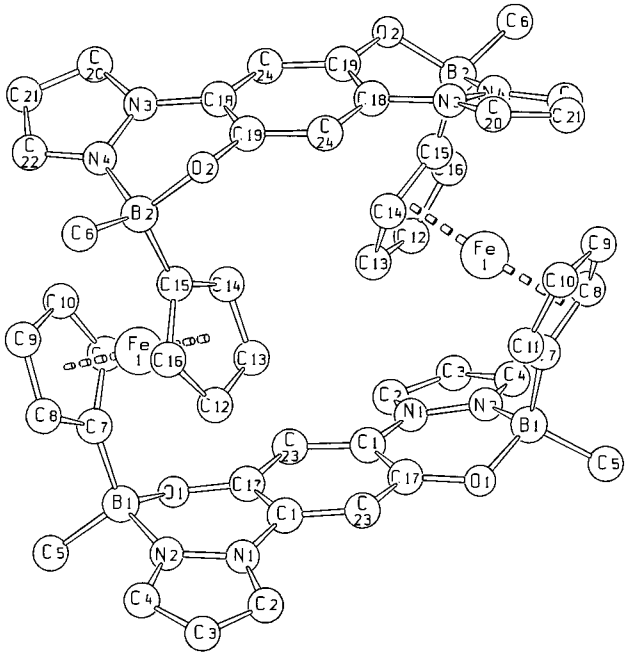

Figure 3. Plot of macrocycle **6**; hydrogen atoms omitted for clarity.

features two 1,1′-disubstituted ferrocenylene units and two 2,5-di(pyrazol-1-yl)hydroquinone groups as integral parts of a macrocyclic framework (Figure 3). The molecular symmetry C_2 of **6** in the crystal is determined by a 2-fold axis running through the centers of the C_6-rings of the two 2,5-di(pyrazol-1-yl)hydroquinone groups. This 2-fold axis is also present in the crystal, doubling the first half of the macrocyclic dimer which lies in the asymmetric unit.

The other three macrocycles in the unit cell are created by the C-centering, the *c*-glide planes, and the inversion centers. The macrocycles themselves are held together by van der Waals forces only. The crystal structure of **6** is densely packed.

A staggered conformation is adopted by the substituted cyclopentadienyl rings of the ferrocene units. The distance between the centers of gravity of the two hydroquinone rings in **6** is 7.9 Å, while the two iron atoms are 6.7 Å apart from each other. Space-filling drawings of **6** show that there is essentially no free space in the interior of the macrocycle.

Each macrocycle **6** contains four chiral boron atoms, all of them possessing the same configuration. The entire sample consists of a racemic mixture of *SSSS* and *RRRR* species.

Conclusion

The ferrocene-containing macrocycle **6** is accessible in high yield from 1,1′-fc[B(Me)NMe$_2$]$_2$ {fc = Fe(C$_5$H$_4$)$_2$} and 2,5-di(pyrazol-1-yl)hydroquinone. The synthesis approach takes advantage of the facile formation of B−O and B−N bonds.

Using high-resolution X-ray powder diffraction, it is nowadays possible to solve crystal structures of organometallics of moderate complexity in a routine manner, once the connectivity between the functional groups is known. In the present case, X-ray powder crystallography was able to verify that cyclic molecules had been generated and to exclude that open-chain polymeric species had been formed. It was, however, not possible to deduce the correct crystal structure from powder data alone. The final structure has basically been obtained from the initial structure solution by straightforward DFT optimizations of **6** and the primitive unit cell. The structural changes brought about by the final rigid body Rietveld refinement are relatively small. It may be concluded that a combination of direct space methods, energy minimization, and rigid body Rietveld refinement is extremely powerful and will further enhance the capabilities of powder diffraction data in the future.

Experimental Details

General Considerations. All reactions and manipulations of air-sensitive compounds were carried out in dry, oxygen-free argon using standard Schlenk ware. CH_2Cl_2 was freshly distilled under N_2 from CaH_2 prior to use. NMR: Bruker DPX 250, Bruker AMX 400 spectrometers. Abbreviations: s = singlet; d = doublet; vt = virtual triplet; n.r. = multiplet expected in the ^{1}H NMR spectrum but not resolved; n.o. = signal not observed; pz = pyrazolyl; hqui = hydroquinone. Elemental analyses were performed by the microanalytical laboratory of the University of Frankfurt.

Synthesis of 6. A CH_2Cl_2 solution (35 mL) of **1** (0.15 g, 0.62 mmol) was added with stirring at room temperature to a solution of **4** (0.20 g, 0.62 mmol) in 15 mL of CH_2Cl_2. The mixture was stirred for 2 days, whereupon yellow microcrystals gradually precipitated while $HNMe_2$ was liberated. The yellow solid material was collected on a frit, triturated with CH_2Cl_2 (15 mL), and dried in vacuo. Yield: 0.25 g (85%). ^{1}H NMR (250.1 MHz, [D$_6$]DMSO): δ 0.26 (s, 12H; BCH_3), 3.24, 3.29, 3.32, 3.41 (4 × n.r., 4 × 4H; C_5H_4), 6.93 (vt, 4H, ^3J(HH) = 2.6 Hz; pz-H4), 7.55 (s, 4H; hqui-C*H*), 8.23, 8.89 (2 × d, 2 × 4H, ^3J(HH) = 2.6 Hz; pz-H3,5). ^{13}C NMR (100.5 MHz, [D$_6$]DMSO): δ 7.34 (B*C*H$_3$), 68.3, 68.6, 69.5, 70.6 (C_5H_4), 107.8 (pz-C4), 108.3 (hqui-*C*H), 123.8 (hqui-CN), 128.5, 134.7 (pz-C3,5), 142.1 (hqui-CO); n.o.: C_5H_4-ipso. Anal. Calcd for $C_{48}H_{44}B_4Fe_2N_8O_4$ (952.87) + 0.5 CH_2Cl_2 (84.93): C, 58.59; H, 4.56; N, 11.27. Found: C, 58.43; H, 4.73; N, 11.16. ESI-MS: *m/z* 952 [M$^+$; 100%].

Electrochemical Measurements on 6. Potential values are referred to the saturated calomel electrode (SCE). Under the experimental conditions applied, the one-electron oxidation of ferrocene occurs at +0.49 V.

Crystal Data of 6. X-ray powder diffraction data were collected for complex **6** at 295 K on beamline X3B1 of the Brookhaven National Synchrotron Light Source (λ = 1.14991(2) Å) in transmission geometry with the sample sealed in a 0.7 mm lithiumborate glass (No. 50) capillary (Table 1). Data reduction was performed using the GUFI[21] program. Indexing with ITO[22] led to a C-centered monoclinic unit cell with lattice parameters given in Table 1. Low-angle reflections had a fwhm of 0.014°2θ, which is significantly broader than the resolution of the spectrometer.

Acknowledgment. This research was supported by the "Deutsche Forschungsgemeinschaft" (DFG) and the "Fonds der Chemischen Industrie" (FCI). L.D. is grateful to the "Alexander von Humboldt Foundation" for a postdoc grant. The authors would like to thank Piero Zanello and Fabrizia Fabrizi de Biani for electrochemical investigations, as well as Niri Govind for his help with the DFT calculations. Research was carried out in part at the National Synchrotron Light Source at Brookhaven National Laboratory, which is supported by the U.S. Department of Energy, Division of Materials Sciences and Division of Chemical Sciences. The SUNY X3 beamline at NSLS is supported by the Division of Basic Energy Sciences of the U.S. Department of Energy under Grant No. DE-FG02-86ER45231.

Supporting Information Available: More details of the structure solution procedure, tables of structure refinement, 2θ values, diffraction intensities, atomic coordinates, bond lengths and angles, anisotropic displacement parameters, and hydrogen coordinates for complex **6**. This material is available free of charge via the Internet at http://pubs.acs.org.

OM0105066

(21) Dinnebier, R. E.; Finger, L. W. *Z. Kristallogr. Suppl.* **1998**, *15*, 148. Obtainable at http://www.pulverdiffraktometrie.de.
(22) Visser, J. W. *J. Appl. Crystallogr.* **1969**, *2*, 89.